Electron-spin resonance investigation of the cation exchange of the semiquinone of 3,3′,4,4′-tetrahydroxybiphenyl

Jens A. Pedersen
Department of Chemistry, University of Aarhus, DK-8000 Aarhus C, Denmark

ESR studies of the semiquinone of 3,3′,4,4′-tetrahydroxybiphenyl in aqueous ethanolic solutions have shown the radical undergoes cation exchange whenever the cation concentration $[Na^+] > 0.02$ mol dm^{-3}. By the two-site exchange, which can be followed completely from no exchange ($[Na^+] = 0.02$ mol dm^{-3}) to fast exchange, the coupling constants of three pairs of protons are interchanged. The fastest exchange observed leads to a correlation time $\tau = 1.43$ ns.

From interactive simulations, based on the density-matrix method in the Alexander–Kaplan formalism, close matches are obtained for all observed spectra. The simulations unequivocally show that two splitting constants out of six are derived from positions with negative spin densities. The simulations also demonstrate that two slightly different radical conformers undergo exchange simultaneously. A temperature study from −40 to 80 °C of one sample, having $[Na^+] = 0.2$ mol dm^{-3}, shows that the splitting constants change with temperature, whereas the correlation time is found to be independent of temperature.

Introduction

Chelate complexes of *o*-benzosemiquinones with a number of metal ions have been known for a long time.[1,2] Thus, Eaton studied the possibility of obtaining stabilised free radicals as well as stabilised valencies of transition metals by formation of complexes.[1] Lucken reported alkali-metal semiquinones in anhydrous *tert*-butyl alcohol (TBA) to form tightly bound ion pairs.[2] The ion pairs were immediately destroyed and 'free' semiquinone radicals were observed by the addition of small amounts of water. Brustolon *et al.*[3] extended the latter study to methyltetrahydrofuran (MTHF). They suggested that the alkali-metal ion is chelated by two oxygens in MTHF whilst the metal is paired to only one in TBA.

While there have been several reports of complexes of *o*-benzosemiquinones and transition- and non-transition-metal ions in non-aqueous solvents,[4] reports on complexes in aqueous solutions are few.

Felix and Sealy[5] generated (photolytically) semiquinone complexes with metal ions from groups 2B, 3A and 3B in aqueous solutions. All ions gave rise to hyperfine splittings, whereas no splittings were observed from metal ions of group 2A.

When one considers complexes in aqueous solutions of *o*-semiquinones and group 1A metals, the absence of observable alkali-metal splittings has made the possible complex structures or their mere existence a matter of dispute. Further, the observation that no significant difference exists between the ring proton constants of a free *o*-semiquinone anion and its salts complicates the discussion further.[2]

We here report ESR studies of the semiquinone of 3,3′,4,4′-tetrahydroxybiphenyl in alcoholic aqueous solutions. The studies lead to new evidence about the interaction between alkali cations and one of the two catechol moieties. They show that the radical undergoes cation exchange, a process which can be followed completely from no exchange to fast exchange. The two-site exchange is, to our knowledge, the first published case, interactively analysed by computer, where the coupling constants of three pairs of protons are interchanged.

ESR studies of symmetrically hydroxy-substituted biphenyls usually exhibit equal distribution of the unpaired electron on both phenyl rings.[4,6,7] For the semiquinone of 3,3′,6,6′-tetrahydroxy-4,4′-dimethoxybiphenyl an equal distribution was observed, when the radical was formed by electrolysis in water, dimethylformamide (DMF) or mixtures thereof. However, when formed in aq. alkali by autoreduction, the unpaired electron was clearly confined to one ring only.[4] Attempts to follow the transition between the two forms in a continuous progress were unsuccessful.

The present study has now demonstrated the progress which can be made using the semiquinone of 3,3′,4,4′-tetrahydroxybiphenyl by varying the NaOH concentration of the aqueous solution.

Experimental

3,3′,4,4′-Tetrahydroxybiphenyl was obtained from ICN Biochemicals, Cleveland and used as obtained. The semiquinone radicals were generated in alkaline aq. ethanol at room temperature by autoxidation: solvent [20 mm^3; 80% alcohol (v/v)] containing the biphenyl was mixed with water (5 mm^3) adjusted with NaOH to a prefixed pH. Varying pH and the sodium-ion concentration in consort was chosen to allow us to obtain spectra for the total range of exchange rates and stable radicals as well.

All spectra were recorded on a Bruker ER200 spectrometer, modulation frequency 25 kHz and amplitude 25 mG. The digitised spectra (4 k, resolution 2.5 mG) were simulated on a Wax 6210 computer as outlined in the next section.

Simulations

The spectra obtained have been intepreted by interactive simulations. In order to obtain comprehensive information from a given spectrum, and to establish the relaxation mechanism for the involved radicals, different types of simulations have been performed by choosing between various options, built into the simulation program, *e.g.*

Option 1a. A traditional simulation with Lorentzian line shape and constant linewidth to all lines. Two or more spectra may be superposed.

Option 1b. An extension is to vary the linewidth to take account of relaxation from *g*- and *A*-tensor anisotropy.[8] The observed asymmetric line broadening is taken into account by introducing formulas in the simulation procedure of the form of eqn. (1).

Table 1 ESR proton splitting constants (a_i/G), linewidths (lw/mG), relative offsets (offs/mG) and intensities (int), and correlation times (τ) from the radical of 3,3′,4,4′-tetrahydroxybiphenyl. Nr. 1–5 are from single-radical simulations, Nr. 1A/1B–5A/5B from double-radical simulations (two conformers)

Nr.	a_2	$a_{2'}$	a_5	$a_{5'}$	a_6	$a_{6'}$	lw	rms	offs	int	τ
1	0.677	−0.396	1.359	−0.182	3.331	1.105	101	100			∞
2	0.631	−0.442	1.351	−0.149	3.339	1.173	99	100			1.84 μs
3	0.609	−0.440	1.346	−0.138	3.333	1.197	94	100			1.16 μs
4	0.711	−0.457	1.432	−0.135	3.538	1.343	83	100			25.22 ns
4′	0.773	−0.477	1.436	−0.133	3.549	1.365	80	100			14.72 ns
4″	0.777	−0.480	1.435	−0.131	3.548	1.366	82	100			14.42 ns
5	0.979	−0.564	1.456	−0.136	3.610	1.406	82	100			1.45 ns
1A	0.676	−0.401	1.357	−0.181	3.331	1.109	94	68	0	100	∞
2A	0.623	−0.454	1.366	−0.158	3.329	1.202	80	68	0	100	1.05 μs
3A	0.605	−0.454	1.341	−0.131	3.335	1.215	73	77	0	100	0.87 μs
4A	0.680	−0.450	1.428	−0.127	3.535	1.329	78	84	0	100	31.26 ns
5A	0.968	−0.567	1.465	−0.123	3.618	1.389	73	93	0	100	1.43 ns
1B	0.682	−0.295	1.346	−0.190	3.325	1.049	92		−33	24	∞
2B	0.647	−0.417	1.363	−0.172	3.324	1.151	110		−20	77	5.09 μs
3B	0.620	−0.427	1.363	−0.161	3.312	1.190	103		−11	93	1.54 μs
4B	0.728	−0.447	1.415	−0.121	3.535	1.365	79		0	78	22.05 ns
5B	0.994	−0.562	1.415	−0.121	3.609	1.418	88		0	90	1.43 ns

$$1/T_2 = A + BM + CM^2 + DMM' \quad (1)$$

Option 2. A simulation to take account of relaxation from cation exchange, based on the Alexander–Kaplan procedure.

The exchange model (*Option 2*) is based on the density matrix formalism given by Alexander[9] and following Kaplan's earlier work.[10] This model has been chosen to allow us to consider the total process from slow to fast exchange. The line shape function is given in the usual way by eqn. (2) where the density matrix

$$f(\omega) = \mathrm{Im}\mathrm{Tr}\{\rho S^+\} = \mathrm{Im}(\sum_{i=1}^{p} \rho_{i+p,i}) \quad (2)$$

elements are obtained from the master equation, formally written as in eqn. (3). The Hamiltonian operator is taken in a

$$\frac{d\rho}{dt} = \frac{1}{i\hbar}[\mathscr{H},\rho] + \left(\frac{d\rho}{dt}\right)_{relax} + \left(\frac{d\rho}{dt}\right)_{exch} \quad (3)$$

rotating coordinate system, *i.e.* eqn. (4) holds. We have made a

$$\mathscr{H}/\hbar = (\omega_o - \omega)S_Z + S_X\omega_1 + \sum_{i=1}^{n} a_i S_Z I_Z i \quad (4)$$

program in which we calculate the matrix elements of eqn. (3), then make the summation (2) to obtain the final line shape. To obtain a 'best set' of parameters the spectrum fitting is performed in an iterative fashion. All parameters for each radical, *i.e.* the hyperfine splittings, the offset, the basic linewidth ($1/T_2$), the correlation time (τ) and the relative amount are changed systematically in small steps by the computer, and the quality of fit was estimated by the mean-square-deviation criteria (rms-value).

From the simulations it turned out that all obtained spectra could be approximately matched by a simulation based on a single radical data set by *Option 2*, we shall arbitrarily scale the rms-values for these single-radical simulations to 100. The rms-value for any other simulation on the same spectrum, *e.g.* involving more than one radical, is then given relative to this figure.

Results

The very first radical we observed in aq. alkali did not reveal a 27-line spectrum as expected, with equal distribution of the unpaired electron between the two phenyl rings, but an anomalous and complex spectrum, containing a mixture of broad and sharp lines [Fig. 1(2a) below]. Attempts to interpret the spectrum were unsuccessful until a simulation made us realise that an exchange process was responsible for the strange spectral observations.

In the following we shall begin discussing the different spectra appearing from the radicals of the title compound, when the Na^+ concentration was varied. All spectra are first interpreted by single-radical exchange simulations using *Option 2*. The simulations are numbered from 1 to 5 in Table 1, where splitting constants, linewidth (lw), relative rms-value and correlation time (τ) are stated for each one. For numbering positions see formula in the Discussion.

Spectrum Nr. 1

This spectrum, shown in Fig. 1(1a), exemplifies the state of no exchange. The sodium cation ([Na^+] = 0.02 mol dm^{-3}, pH of the solution ~ 12.3) is tightly positioned somewhere between two oxygen atoms of one ring, leading to an asymmetric radical.

An exchange simulation of the spectrum (*Option 2*) based on a radical with 6 different splitting constants (64 lines) yields a fair match of the 40 lines seen (Table 1, Nr. 1). However, careful inspection shows features which we have been unable to match by a single-radical simulation, *e.g.* in the experimental spectrum the two-times-two lines marked with stars exhibit single-line counterparts (see the symmetrically positioned lines marked with double stars).

Accordingly, we are dealing with two radicals, which we shall term the A and the B conformer, respectively. A renewed exchange simulation based on the data for conformers 1A and 1B (Table 1) leads to a close match between the experimental and the simulated spectra [Figs. 1(1a) and 1(1b)] and an rms-value of 68. We thus observe a 32% better fit relative to the one based on a single radical.

We obtained identical splitting constants for 1A and 1B and the same rms-value, whether we simulate using *Option 1a* with constant linewidth or *Option 2* with exchange, respectively. In fact, when introducing an exchange broadening ($1/\tau > 0$) in the latter case the iteration eventually leads to no broadening ($\tau \longrightarrow \infty$). Accordingly, we have no confirmation from spectrum 1 that exchange broadening actually takes place.

Spectrum Nr. 2

When increasing the cation concentration to [Na^+] = 0.06 mol dm^{-3}, with a pH of about 12.8, the observed spectrum [Fig.

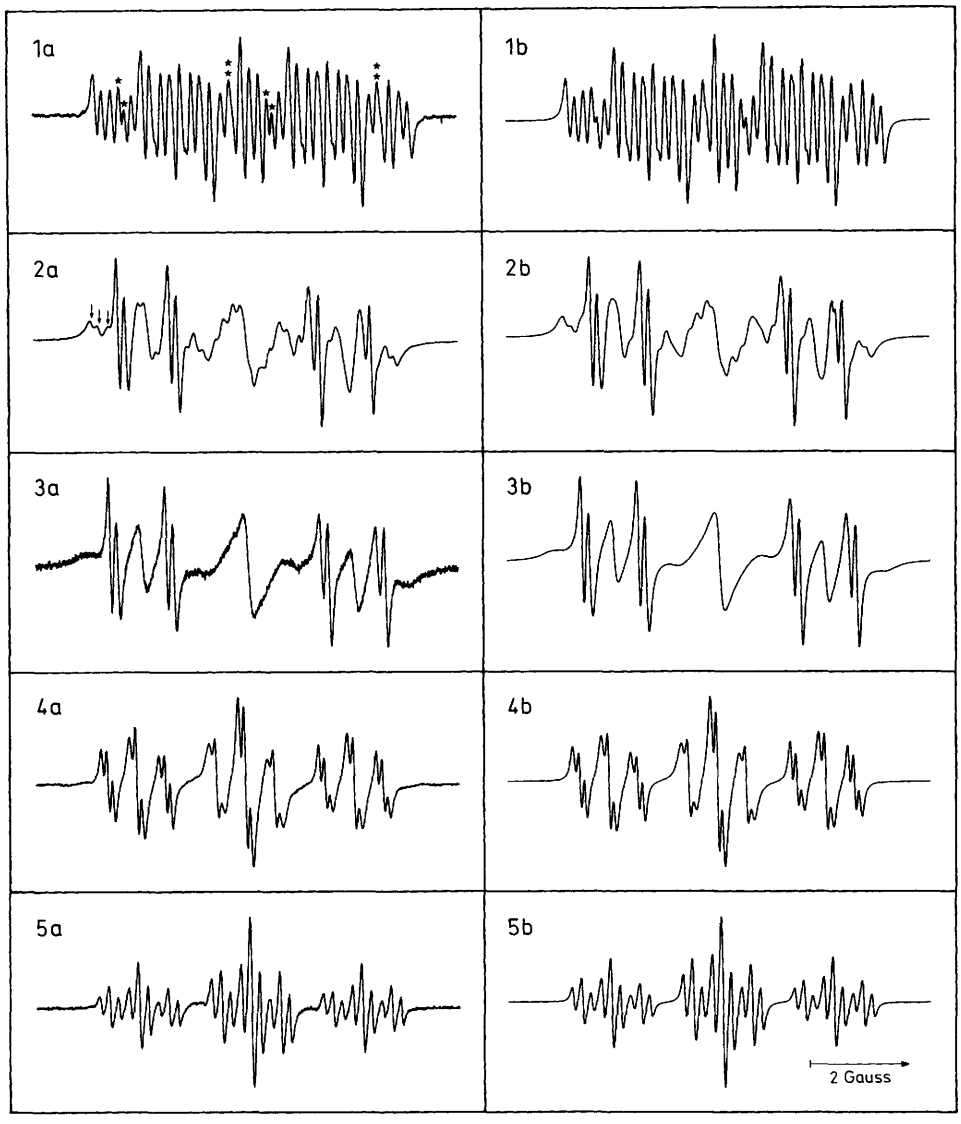

Fig. 1 The ESR spectra of radicals from 3,3′,4,4′-tetrahydroxybiphenyl (1a–5a) and their simulated counterparts (1b–5b). For details, see text.

1(2a)] exhibited marked line broadening. Eight lines stayed sharp, while all other lines were drastically decreased in intensity. By use of a single set of data (Table 1, Nr. 2) and including exchange in the simulation the main spectral features were covered. A close match, however, was obtainable only by incorporating two sets of data (see Nr. 2A and 2B), as was demonstrated from comparison of Fig. 1(2a) and 1(2b), and noticing the fit again improves by 32%.

The simulation yielded correlation times of 1.05 and 5.09 μs for 2A and 2B, respectively.

Fig. 1(2a) shows three broad lines (see arrows) to the left of the first sharp line. This feature unequivocally demonstrates that two splitting constants are derived from protons at positions with negative spin densities. This is completely in line with the chosen simulation, where a close match is obtainable only when two splitting constants are given the opposite sign of the remaining four constants.

Notice that we apply the incorrect but common practice of considering proton splitting constants as positive for positive spins. In assigning the splitting constants, we are first guided by the fact that we know which pair of constants exchange in the process; secondly we utilise known assignments given to other 4-substituted catechol semiquinones.[4]

Spectrum Nr. 3

The complexity of the present reaction was demonstrated when considering the spectrum of Fig. 1(3a). It was obtained from a sample made up in the same way as that giving rise to Fig. 1(2a), the only difference being that Fig. 1(3a) was obtained a few minutes after mixing, whereas Fig. 1(2a) was obtained several minutes after mixing. From the simulation (Table 1) it appeared that the splitting constants and correlation times for the A plus B conformers of Fig. 1(3a) were very close to the corresponding values obtained from Fig. 1(2a). We observed a slightly faster exchange rate for 3A and 3B than for 2A and 2B.

In order to test the correctness of the obtained constants we have applied the following relation (5), which follows from the theory.

$$d_i(8) = a_i + a_{i'} \; (i = 2, 5, 6) \qquad (5)$$

The constants/distances on the left were obtained from a simulation with constant linewidth of the eight sharp lines of Fig. 1(2a) and 1(3a). They are shown in Table 2, both for a single eight-lines simulation and for a double eight-lines simulation (A and B). These figures were then compared with

Table 2 ESR proton splitting constants (a_i/G) or distances (d_i/G), linewidths (lw/mG), and relative intensities (int) obtained as described in the text. The splitting constants are compared with sums obtained from Table 1 [*cf.* eqns. (5) and (6)].

Nr.	d_2 (8)	($a_2 + a_{2'}$)	d_5 (8)	($a_5 + a_{5'}$)	d_6 (8)	($a_6 + a_{6'}$)	lw/mG	int
2	0.183	(0.189)	1.204	(1.202)	4.516	(4.512)	88	
3	0.168	(0.169)	1.208	(1.208)	4.529	(4.530)	87	
	$2a_2$ (27)		$2a_5$ (27)		$2a_6$ (27)			
4	0.256	(0.254)	1.298	(1.297)	4.882	(4.881)	102	
4′	0.296	(0.296)	1.302	(1.303)	4.914	(4.914)	102	
4″	0.296	(0.297)	1.304	(1.304)	4.914	(4.914)	97	
5	0.406	(0.415)	1.288	(1.320)	4.896	(5.016)	83	
	d_2 (8)		d_5 (8)		d_6 (8)			
2A	0.161	(0.169)	1.212	(1.208)	4.539	(4.531)	83	100
2B	0.211	(0.230)	1.193	(1.191)	4.487	(4.475)	72	74
3A	0.151	(0.151)	1.212	(1.210)	4.555	(4.550)	79	100
3B	0.185	(0.193)	1.205	(1.202)	4.504	(4.502)	81	92
	$2a_2$ (27)		$2a_5$ (27)		$2a_6$ (27)			
4A	0.256	(0.230)	1.298	(1.301)	4.882	(4.864)	76	100
4B	0.258	(0.281)	1.290	(1.294)	4.876	(4.899)	164	74
5A	0.398	(0.401)	1.334	(1.342)	5.008	(5.007)	82	100
5B	0.434	(0.432)	1.302	(1.294)	5.026	(5.027)	84	88

Table 3 ESR proton splitting constants (a_i/G), and linewidths (lw/mG) as a function of temperature obtained from *Option 1* simulations of the spectra of Fig. 2. The splitting constants are compared with sums obtained from Table 4 [*cf.* eqn. (6)].

Nr.	T/°C	a_2 (27)	($a_2 + a_{2'}$)/2	a_5 (27)	($a_5 + a_{5'}$)/2	a_6 (27)	($a_6 + a_{6'}$)/2	lw/mG
1T	−30.8	0.089		0.670		2.397		668
2T	−21.6	0.127		0.669		2.414		442
3T	−11.1	0.186		0.641		2.418		219
4T	0.8	0.165	(0.161)	0.635	(0.637)	2.413	(2.412)	142
5T	12.5	0.135	(0.136)	0.635	(0.635)	2.392	(2.394)	98
6T	25.6	0.122	(0.122)	0.633	(0.633)	2.382	(2.382)	94
7T	41.0	0.099	(0.097)	0.629	(0.629)	2.363	(2.363)	88
8T	52.8	0.080	(0.079)	0.626	(0.627)	2.346	(2.346)	93
9T	64.7	0.040	(0.060)	0.622	(0.626)	2.331	(2.335)	122
10T	76.4	0.016	(0.040)	0.619	(0.624)	2.319	(2.318)	120
11T	80.0	0.011	(0.030)	0.617	(0.619)	2.308	(2.308)	95

the constants to the right in eqn. (2) obtained as the sum of each pair of exchanging 'proton constants', given the correct sign. We observed an excellent correspondence.

Spectrum Nr. 4

Increasing the sodium cation concentration to 0.2 mol dm^{-3} made the radical which yielded a 27-line spectrum, Fig. 1(4a). Simulating this fast exchange broadened spectrum as derived from a single radical gave rise to the constants Nr. 4 in Table 1. A 16% better fit was obtained, when basing the simulation on two sets of data (Nr. 4A and 4B). The spectrum of Fig. 1(4b) is a close match to Fig. 1(4a). The correlation times have decreased relative to those of radical Nr. 3 to 31.26 and 22.05 ns for 4A and 4B, respectively, or to 25.22 ns for the single-radical simulation.

If we ran the very same sample 57 min later, we obtained a spectrum (not shown) seemingly identical with that of Fig. 1(4a). If we compare the obtained simulation data (Nr. 4′), however, we see that the correlation time has dropped to 14.72 ns; for simplicity only single-radical data are considered (Nr. 4, 4′ and 4″). Thus, not only do the splitting constants change, but the correlation time eventually decreases from 25.22 ns (Nr. 4) to 14.72 ns (Nr. 4′); continuing the measurement 12 h later, for this extremely stable sample, leads to a nearly unchanged correlation time of 14.42 ns (Nr. 4″). We have no explanation of this behaviour at present.

Spectrum Nr. 5

Finally, when increasing the pH > 14 the spectrum of Fig. 1(5a) was observed. This spectrum exhibited the fastest exchange we have been able to observe, with a correlation time of 1.43 ns. When the simulation was based on a double set the fit improved by 7% only. Further, we observed nearly identical values for τ, 1.45 ns for Nr. 5 and 1.43 ns for 5A and 5B.

In line with the testing applied above [eqn. (5)], we have used the following eqn. (6) for 27-line spectra, Figs. 1(4a) and

$$2a_i(27) = a_i + a_{i'} \; (i = 2, 5, 6) \qquad (6)$$

(5a). It implies that the splitting constants from a 27-line spectrum taken twice is equal to the sum of corresponding constants of an exchanging pair of protons. Table 2 demonstrates this condition to be fulfilled.

Temperature studies

In order to gain further insight into the mechanism behind the exchange process, we made a preliminary temperature study of one sample, having [Na^+] = 0.2 mol dm^{-3} and a pH ~ 13.3. We were able to keep the radicals and to run the sample, from −40 to 80 °C. The eleven spectra, numbered 1T to 11T, were all of the 27-line type. Only eight spectra are shown in Fig. 2.

To obtain an overview of the observed changes, we first made a simulation by way of one set of 3-times-2-proton constants, and constant linewidth, *Option 1a*. The obtained data, shown in Table 3 under the headings a_i(27), exhibited a systematic change

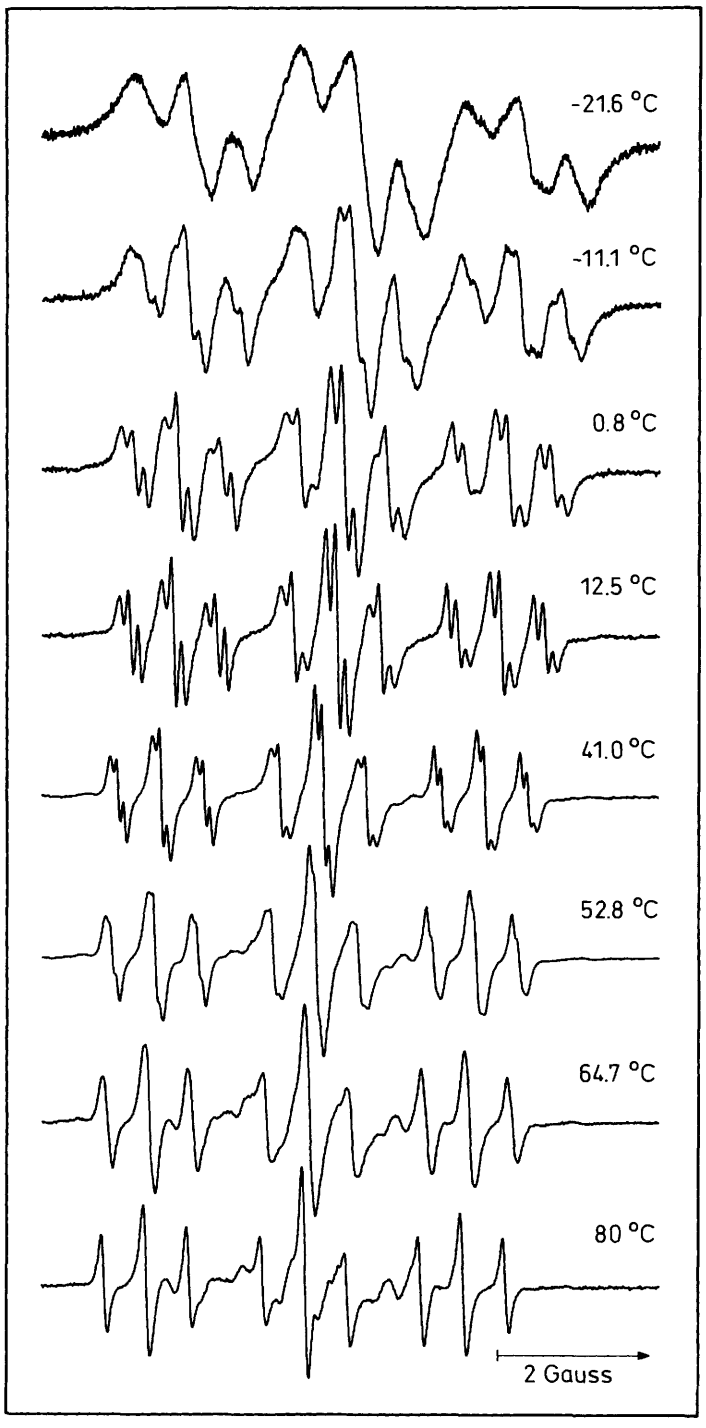

Fig. 2 The ESR spectra of radicals from 3,3′,4,4′-tetrahydroxybiphenyl as a function of temperature. Notice the extra lines in the spectrum at 41 °C and in those at higher temperatures. They derive from generated secondary products. For details, see text.

from about 2 °C, when lowering the temperature. When using the exchange program we were unable to obtain reliable simulations for spectra below 0 °C. We shall accordingly focus on those run at positive temperatures.

Since two radical conformers give rise to the exchange broadened spectra, we have used two sets of data in the final simulations. The obtained results are shown in Table 4.

From a glance at the relative intensities (int) we observed that the B-conformer fades away when the temperature is increased. The set of data for 10TB and 11TB might be unrealistic, in view of relative offsets, the small relative intensities, and not least the large linewidths found. We shall point out that extra lines arise in the spectra from about 40 °C and upwards. They stem from radicals of secondary products generated at these elevated temperatures. These lines are not accounted for in the simulations.

Concerning the splitting constants, two were found to have opposite signs compared with the remaining four, in line with our previous finding. We have made a comparison with the help of eqn. (6) between the simulations performed with constant linewidth and those performed with the exchange facility. The satisfactory result is shown in Table 3.

The observed correlation times for the sample considered were found to be independent of temperature, *i.e.* the exchange processes have zero activation energy for both conformers. This finding is based on analysis very close to the fast-exchange limit. More firm conclusions about the temperature dependence of the present system might be obtainable from studies at lower $[Na^+]$ concentrations.

Discussion

The data reported here have demonstrated that the title compound undergoes cation exchange in aq. ethanol at an elevated pH, when $[Na^+] > 0.02$ mol dm^{-3}. For $[Na^+] = 0.02$ mol dm^{-3} (pH $\approx$ 12.3) exchange was not observed ($\tau \longrightarrow \infty$), but the two catechol units were found to be non-identical. A stable complex between one of the units and one sodium cation has been created, making the biphenyl asymmetric.

For all samples studied the simulations unequivocally demonstrated two radicals to be present, apart from at elevated temperatures. From the fact that the catechol units are non-coplanar and that the two radicals in a sample yielded only slightly different coupling constants the radicals might correspond to *cis* and *trans* isomers of the biphenyl. Their exact structures, however, cannot be deduced from the present data, only that interconversion between the isomers seems slow on the ESR time-scale.

The exchange reaction can formally be described for each isomer by a reaction scheme of the form as shown in Scheme 1.

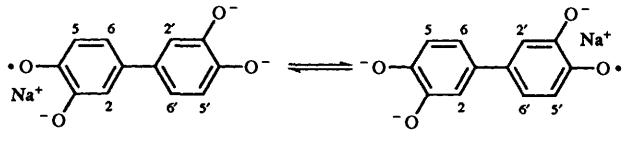

Scheme 1

The cation exchange is likely to be intermolecular, and takes place with another cation source in the solution attaching a different site of the radical. The unpaired electron is then shifted simultaneously with the same rate, in an intramolecular process.[11]

Detailed simulations on Fig. 1(1a) indicate that an extra splitting is discernible, apart from the 6 already reported. Thus, a renewed simulation with two radicals and constant linewidth, including an extra small splitting with spin = 3/2 (Na^+), leads to the following additional data:

1A: lw = 76 mG (before = 90 mG) and a_{Na} = 19 mG
1B: lw = 71 mG (before = 100 mG) and a_{Na} = 21 mG
rms = 63, a 5% improvement

Changing the spin of the small splitting to 1/2 (this could be explained as being derived from an undissociated OH proton) the simulation yields:

Table 4 ESR proton splitting constants (a_i/G), linewidths (lw/mG), relative offsets (offs/mG) and intensities (int), and correlation times (τ) as a function of temperature from the two radical conformers of 3,3′,4,4′-tetrahydroxybiphenyl

Nr.	a_2	$a_{2'}$	a_5	$a_{5'}$	a_6	$a_{6'}$	lw	Int	offs	τ/ns
4TA	0.701	−0.422	1.400	−0.112	3.433	1.359	105	100	0	45.26
5TA	0.645	−0.404	1.366	−0.096	3.388	1.375	74	100	0	36.13
6TA	0.573	−0.357	1.327	−0.061	3.387	1.355	76	100	0	37.99
7TA	0.543	−0.374	1.318	−0.061	3.369	1.336	71	100	0	35.63
8TA	0.500	−0.368	1.293	−0.043	3.351	1.327	77	100	0	39.96
9TA	0.475	−0.380	1.283	−0.038	3.344	1.307	79	100	0	45.10
10TA	0.470	−0.391	1.264	−0.016	3.336	1.300	67	100	0	36.22
11TA	0.463	−0.404	1.267	−0.029	3.322	1.295	59	100	0	31.87
4TB	0.726	−0.362	1.335	−0.076	3.451	1.403	112	78	0	24.91
5TB	0.656	−0.354	1.359	−0.092	3.426	1.385	75	70	4	18.85
6TB	0.609	−0.339	1.317	−0.052	3.389	1.396	66	70	0	17.78
7TB	0.576	−0.357	1.317	−0.056	3.369	1.376	62	59	3	16.38
8TB	0.542	−0.359	1.292	−0.036	3.351	1.365	67	52	2	16.55
9TB	0.512	−0.369	1.263	−0.006	3.355	1.336	70	43	7	21.15
10TB	0.465	−0.465	1.238	−0.076	3.246	1.396	202	16	18	13.18
11TB	0.488	−0.393	1.269	−0.088	3.212	1.380	330	6	35	15.86

1A: lw = 79 mG and a_{OH} = 39 mG
1B: lw = 76 mG and a_{OH} = 43 mG
rms = 63

It is our general experience that splitting constants of spin 1/2 nuclei found equal to the linewidth or slightly less, are correctly determined from simulations with constant linewidth. When the splittings become less than the linewidth, there is an increasing tendency that these 'hidden' constants are underestimated.

In Scheme 1, shown above, the semiquinone radical is given three negative charges, corresponding to dissociation of all four hydroxy protons and subsequent oxidation by molecular oxygen. Complete dissociation is expected considering the elevated pH ($\geqslant$12.3) and from the fact that we have observed a poorly resolved spectrum at pH = 11.3, completely different from any of those shown in Fig. 1. This spectrum, which awaits its final analysis, might be derived from a partly dissociated radical.

Further conclusions about the structures of the observed isomers and mechanism of the exchange process cannot be deduced with confidence, unless additional investigations are performed, including rather time-consuming simulations.

Finally, for all exchange-broadened spectra the simulations unequivocally show that two splitting constants are derived from positions with negative spin densities. From a preliminary ENDOR/triple study on a 64-lines spectrum, we have obtained the following set of data:

$$+3.24,\ +1.34,\ \pm 1.22,\ +0.66,\ \pm 0.44,\ -0.18\ \text{G}$$

Firm evidence showed the smallest splitting to have the opposite sign of all other splittings, apart from the splittings 1.22 and 0.44, where the triple resonance spectrum gave a dubious result.

Acknowledgements

We thank Ulrick Kläning for stimulating discussions. The work was supported by a grant from the Aarhus University Research Foundation.

References

1 D. R. Eaton, *Inorg. Chem.*, 1964, **3**, 1268.
2 E. A. C. Lucken, *J. Chem. Soc.*, 1964, 4234.
3 M. Brustolon, L. Pasimeni and C. Corvaja, *J. Chem. Soc., Faraday Trans. 2*, 1975, **71**, 193.
4 J. A. Pedersen, *Handbook of EPR Spectra from Natural and Synthetic Quinones and Quinols*, CRC Press, Boca Raton, Florida, 1985, Tables I.19–20 and IV.
5 C. C. Felix and R. C. Sealy, *J. Am. Chem. Soc.*, 1982, **104**, 1555.
6 E. W. Stone and A. H. Maki, *J. Chem. Phys.*, 1964, **41**, 284.
7 J. Petránek, J. Pilár and O. Ryba, *Collect. Czech. Chem. Commun.*, 1970, **35**, 2571.
8 J. Freed and G. K. Fraenkel, *J. Chem. Phys.*, 1963, **39**, 326.
9 S. Alexander, *J. Chem. Phys.*, 1962, **37**, 967, 974.
10 J. Kaplan, *J. Chem. Phys.*, 1958, **28**, 278; **29**, 462.
11 R. F. Adams and N. M. Atherton, *Chem. Phys. Lett.*, 1967, **1**, 351.

Paper 5/02057C
Received 31*st March* 1995
Accepted 22*nd May* 1995